Automatic Modulation Recognition for Aeronautical Telemetry

Jacob Frogget and Michael Rice
Brigham Young University
Provo, Utah, USA

ABSTRACT

This paper applies the Bianchi-Loubaton-Sirven technique to classification algorithm capable of distinguishing between PCM/FM and SOQPSK-TG. A happy byproduct of the classification algorithm is a reasonably accurate estimate of the bit rate. The classifier is based on the observation that CPM with an integer modulation index contains harmonics at multiples of the symbol rate. The algorithm is based on the CPM representations of PCM/FM and SOQPSK-TG and leverages the property that applying a g-order nonlinearity to any CPM creates a new CPM with modulation index g times the original modulation index. No prior knowledge of the data is assumed. The technique is applied to distinguish between PCM/FM and SOQPSK-TG. Simulation results show that the classifier works essentially error-free for signal-to-noise ratios above 20 dB and for sufficiently high resolution in the search algorithms required by the maximizations.

INTRODUCTION

Automatic modulation recognition has applications ranging from communication interception to cognitive radio. This paper explores the application of these techniques to the modulations used in aeronautical telemetry. Given the scenario where an aircraft or missile is authorized to transmit at a given bit rate using either PCM/FM or SOQPSK-TG, a technician could use this tool to verify that the transmitter has been set up correctly and is operating properly.

A variety of methods for modulation recognition have been described in the open literature. Overviews can be found in [1, 2, 3]. Higher order statistics were used as classifiers in [4, 5, 6, 7]. These were most effective for QAM, MSK, and MFSK. Spooner et al [8, 9] describe the use of cyclic cumulants as a classifier and show that this approach is effective for QAM and PSK. Vito et al [7]

and Dubuc et al [10] apply the kurtosis coefficient of the instantaneous frequency to distinguish between digital FM and analog FM. A problem closely related to classifiers is blind estimation of the symbol rate for a digitally modulated carrier. Of particular interest are blind symbol rate estimators for CPM signals. For CPM signals, blind symbol rate estimators are usually based on statistics with cyclic components as described in [11, 12, 13].

This paper explores the application of the Bianchi-Loubaton-Sirven algorithm [13] (hereafter called the "Bianchi algorithm") to distinguish between PCM/FM and SOQPSK-TG. Because the Bianchi algorithm only works for CPM signals, the CPM representation of PCM/FM and SOQPSK-TG are defined and used. A description of the recognition and estimation algorithm is given as well as simulation results to demonstrate its effectiveness. An interesting by-product of the classifier is an estimate of the bit rate. The accuracy of the bit rate estimator is also presented.

CPM REPRESENTATION OF MODULATIONS USED IN AERONAUTICAL TELEMETRY

Both PCM/FM and SOQPSK-TG can be thought of as special cases of continuous phase modulation (CPM). The complex-valued (I/Q) representation for CPM is

$$s(t) = \exp\{j\phi(t)\} \tag{1}$$

where the phase, $\phi(t)$ is a pulse train expressed as

$$\phi(t) = 2\pi h \sum_k a(k) g(t - kT_s) \tag{2}$$

where T_s is the symbol period ($1/T_s$ is the symbol rate); h is the digital modulation index that quantifies the phase shift for each symbol; and $g(t)$ is the phase pulse that is usually thought of as the time integral of a frequency pulse $f(t)$ that spans L symbols. The convention [14] is to normalize $f(t)$ to have area $1/2$ so that $g(t) = 1/2$ for $t \geq LT_s$. In the CPM literature, modulations with $L = 1$ are called *full response* CPM whereas modulations with $L > 1$ are called *partial response* CPM.

PCM/FM may be expressed as a CPM. The elements of (2) are defined as follows. If $b(k) \in \{0, 1\}$ be the k-th bit, then the $a(k)$ are related to the bits via the mapping

$$a(k) = \begin{cases} -1 & b(k) = 0 \\ +1 & b(k) = 1. \end{cases} \tag{3}$$

The modulation index is $h = 0.7$ and the frequency pulse is

$$f(t) = \begin{cases} \frac{1}{4T_b}\left[1 - \cos\left(\frac{\pi t}{T_b}\right)\right] & -T_b \le t \le T_b \\ 0 & \text{otherwise.} \end{cases} \tag{4}$$

The frequency pulse is plotted in Figure 1. Note that $L = 2$ for PCM/FM.

SOQPSK-TG may also be expressed as a partial response CPM. The elements of (2) are defined as follows: The relationship between the k-th bit $b(k) \in \{0, 1\}$ and the "symbol" $a(k)$ involves a binary-to-ternary mapping. First define

$$u(k) = \begin{cases} -1 & b(k) = 0 \\ +1 & b(k) = 1. \end{cases} \tag{5}$$

The k-th "symbol" $a(k)$ is given by

$$a(k) = (-1)^{k+1} \frac{u(k-1)[u(k) - u(k-2)]}{2}. \tag{6}$$

This produces a constrained ternary output $a(k) \in \{-1, 0, +1\}$. Note that each new $b(k)$ produces a new $a(k)$. Consequently, the $a(k)$ and $b(k)$ are produced at the same rate so that the "symbol rate" and the "bit rate" are the same. The modulation index is $h = 1/2$. The frequency pulse is a spectral raised cosine windowed by a temporal raised cosine:

$$f(t) = C \frac{\cos\left(\frac{\pi \rho B t}{2T_b}\right)}{1 - 4\left(\frac{\rho B t}{2T_b}\right)^2} \times \frac{\sin\left(\frac{\pi B t}{2T_b}\right)}{\frac{\pi B t}{2T_b}} \times w(t) \tag{7}$$

$$w(t) = \begin{cases} 1 & 0 \le \left|\frac{t}{2T_b}\right| < T_1 \\ \frac{1}{2}\left[1 + \cos\left(\frac{\pi}{T_2}\left(\frac{t}{2T_b} - T_1\right)\right)\right] & T_1 \le \left|\frac{t}{2T_b}\right| \le T_1 + T_2 \\ 0 & \text{otherwise} \end{cases} \tag{8}$$

where C is a constant to make the area of $f(t)$ one-half. The four constants involved in the frequency pulse are

$$\rho = 0.7, B = 1.25, T_1 = 1.5, T_2 = 0.5 \tag{9}$$

This produces a partial response pulse shape with $L = 8$. This frequency pulse is also plotted in Figure 1.

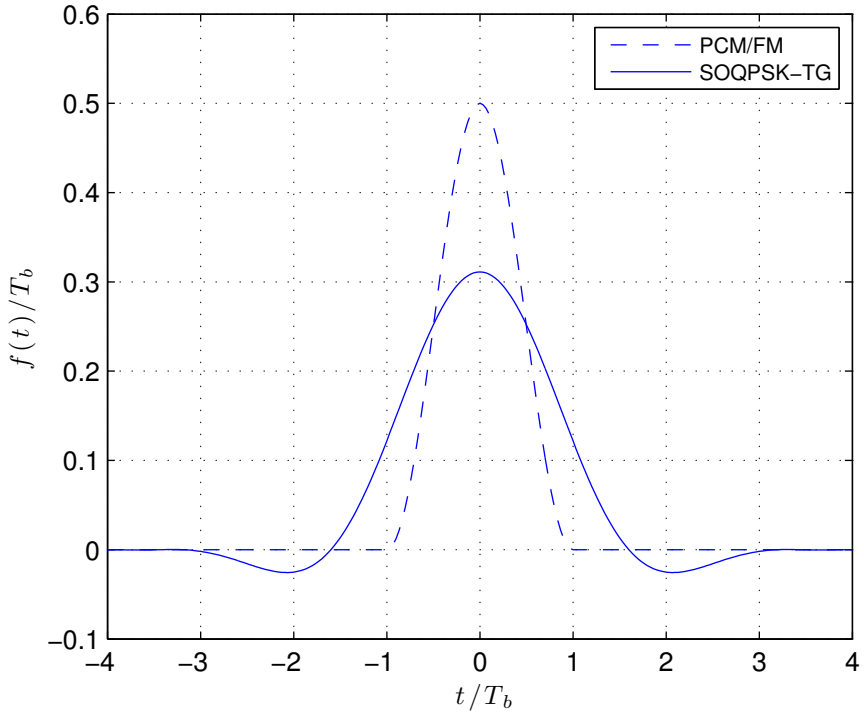

Figure 1: The frequency pulses for PCM/FM and SOQPSK-TG.

THE BIANCHI MODULATION RECOGNITION TECHNIQUE

For automatic recognition, the receiver observes

$$y(t) = s(t-\tau)e^{j2\pi\delta f_0 t} + n(t) \tag{10}$$

and processes the observation $y(t)$ to determine if $s(t)$ corresponds to PCM/FM or SOQPSK-TG. In (10), τ is an known delay, δf_0 is the uncompensated frequency offset in Hz, and $n(t)$ models the additive thermal noise and is a complex-valued Gaussian random process with zero mean and autocovariance function

$$\frac{1}{2}\mathrm{E}\left\{n(t)n^*(t-\tau)\right\} = N_0\delta(\tau). \tag{11}$$

After experimenting with several of the different automatic recognition techniques, we discovered that the Bianchi-Loubaton-Sirven technique [13] produced the most reliable results to distinguish between PCM/FM and SOQPSK-TG. This technique is based on the following line of reasoning. Let $s(t)$ be a CPM signal with modulation index h:

$$s(t) = e^{j2\pi h\sum_k a(k)g(t-kT_s)} \tag{12}$$

and let g be a positive real number. Now form $s^g(t)$. This may be expressed as

$$s^g(t) = \left(e^{j2\pi h\sum_k a(k)g(t-kT_s)}\right)^g = e^{j2\pi hg\sum_k a(k)g(t-kT_s)}. \tag{13}$$

This shows that $s^g(t)$ is a new CPM signal with modulation index hg. The recognition algorithm is based on the following observations:

- if $hg \neq$ integer, then $\mathrm{E}\{s^g(t)\} = 0$.
- if $hg =$ even integer, then $\mathrm{E}\{s^g(t)\}$ is periodic with period T_s.
- if $hg =$ odd integer, then $\mathrm{E}\{s^g(t)\}$ is peroidic with period $2T_s$, but only the odd harmonics are present.

These observations are neatly captured in the function

$$r(g,\alpha) = \lim_{T\to+\infty} \frac{1}{T} \int_0^T \mathrm{E}\left\{s^g(t) e^{-j2\pi\alpha t}\right\} dt \tag{14}$$

where $\mathrm{E}\{\cdot\}$ is the statistical expectation operator. Based on the observations regarding hg, $r(g,\alpha)$ is non-zero if and only if hg is an integer. If hg is an even integer, then the periodicity of $\mathrm{E}\{s^g(t)\}$ produces peaks in $r(g,\alpha)$ when α is an integer multiple of $1/T_s$. Similarly, when hg is an odd integer, then the periodicity of $\mathrm{E}\{s^g(t)\}$ produces peaks in $r(g,\alpha)$ when α is an odd-integer multiple of $1/2T_s$.

Now, as stated above, the recognition algorithm operates on $y(t)$ rather than $s(t)$. Thus, the function $r(g,\alpha)$ is defined in terms of $y(t)$ instead of $s(t)$:

$$r(g,\alpha) = \lim_{T\to+\infty} \frac{1}{T} \int_0^T \mathrm{E}\left\{y^g(t) e^{-j2\pi\alpha t}\right\} dt \tag{15}$$

In a practical implementation, the automatic recognition algorithm operates on a sampled version of $y(t)$. Let $y(k)$ be the k-th sample of $y(t)$ and suppose N samples are available for processing. In this case, the function (15) is replaced by [13]

$$r_N(g,\alpha) = \frac{1}{N} \sum_{k=0}^{N-1} \left[\frac{y(k)}{|y(k)|}\right]^g e^{-j2\pi\alpha k} \tag{16}$$

In the noiseless case, $y(k) = y(k)/|y(k)|$. This normalization helps to regulate influence from noise. The function $r_N(g,\alpha)$ is maximized when g is an integer multiple of the modulation index and α is a multiple of the *normalized* symbol rate (ratio of symbol rate to sample rate) as described above. Note that in addition to estimating the modulation index, this algorithm also estimates the bit rate. In the next section, this algorithm is applied to the recognition problem for PCM/FM and SOQPSK-TG.

A MODULATION RECOGNITION ALGORITHM FOR AERONAUTICAL TELEMETRY

The first step in applying the Bianchi technique to the aeronautical telemetry problem is to evaluate $r_N(g, \alpha)$ at values of g that are integer multiples of reciprocals of the two modulation indexes ($h = 0.7$ for PCM/FM and $h = 0.5$ for SOQPSK-TG). The question is, do we use an even multiple of the reciprocal modulation indexes or an odd multiple? In the first case, $r_N(g, \alpha)$ will display a periodic component at the bit rate. In the second case, $r_N(g, \alpha)$ will display a periodic component at odd multiples of half the bit rate. In the original work, Bianchi [13] preferred the second case (that is, $g = 1/h$). This worked best for full response CPM. Indeed, Bianchi pointed out that his approach was best suited for full response CPM and speculated that it would not work well for partial response CPM. Our results show that the Bianchi approach does work for PCM/FM and SOQPSK-TG (both partial response CPM) when $g = 2/h$.

The algorithm is outlined as follows. Let $y(k)$ for $k = 0, 1, \ldots N-1$ be the N samples of the received waveform and let $g_0 = 2/0.7$ (this is for PCM/FM) and let $g_1 = 2/0.5 = 4$ (this is for SOQPSK-TG). Now find

$$R_0 = \max_{\alpha} \left\{ r_N(g_0, \alpha) \right\} \qquad \hat{\alpha}_0 = \operatorname*{argmax}_{\alpha} \left\{ r_N(g_0, \alpha) \right\} \tag{17}$$

$$R_1 = \max_{\alpha} \left\{ r_N(g_1, \alpha) \right\} \qquad \hat{\alpha}_1 = \operatorname*{argmax}_{\alpha} \left\{ r_N(g_1, \alpha) \right\}. \tag{18}$$

Finally, the decision is:

$$\text{modulation} = \begin{cases} \text{PCM/FM with bit rate } \hat{\alpha}_0 \times \text{sample rate} & R_0 \geq R_1 \\ \text{SOQPSK-TG with bit rate } \hat{\alpha}_1 \times \text{sample rate} & R_0 < R_1. \end{cases} \tag{19}$$

A simple illustration of the concept is given in Figure 2. In Figure 2 (a), the input samples $y(n)$ are samples of PCM/FM with an equivalent sample rate of 20 samples/bit. Here, both $|r_N(g_0, \alpha)|^2$ and $|r_N(g_1, \alpha)|^2$ are plotted as a function of α. We observe a peak in $|r_N(g_0, \alpha)|^2$ at $\alpha = 0.05$ bits/sample corresponding to the normalized bit rate of $1/20 = 0.05$ bits/sample. There are peaks in $|r_N(g_1, \alpha)|^2$ as well, but none of these peaks are as high as the peak in $|r_N(g_0, \alpha)|^2$. In Figure 2 (b), the $y(n)$ are samples of SOQPSK-TG with an equivalent sample rate of 20 samples/bit. There is a peak in $|r_N(g_1, \alpha)|^2$ at $\alpha = 1/20$ as expected and this peak is higher than any peak in $|r_N(g_0, \alpha)|^2$. The most noticeable feature here is the very strong peak at $|r_N(g_1, 0)|^2$. The negative consequence of this is that (18) will *always* give $\hat{\alpha}_1 = 0$ and $R_1 > R_0$ when the true signal is SOQPSK-TG. While the decision may be correct, the bit rate estimate is very bad. To fix this problem, the searches (17) and (18) omit the region around $\alpha = 0$.

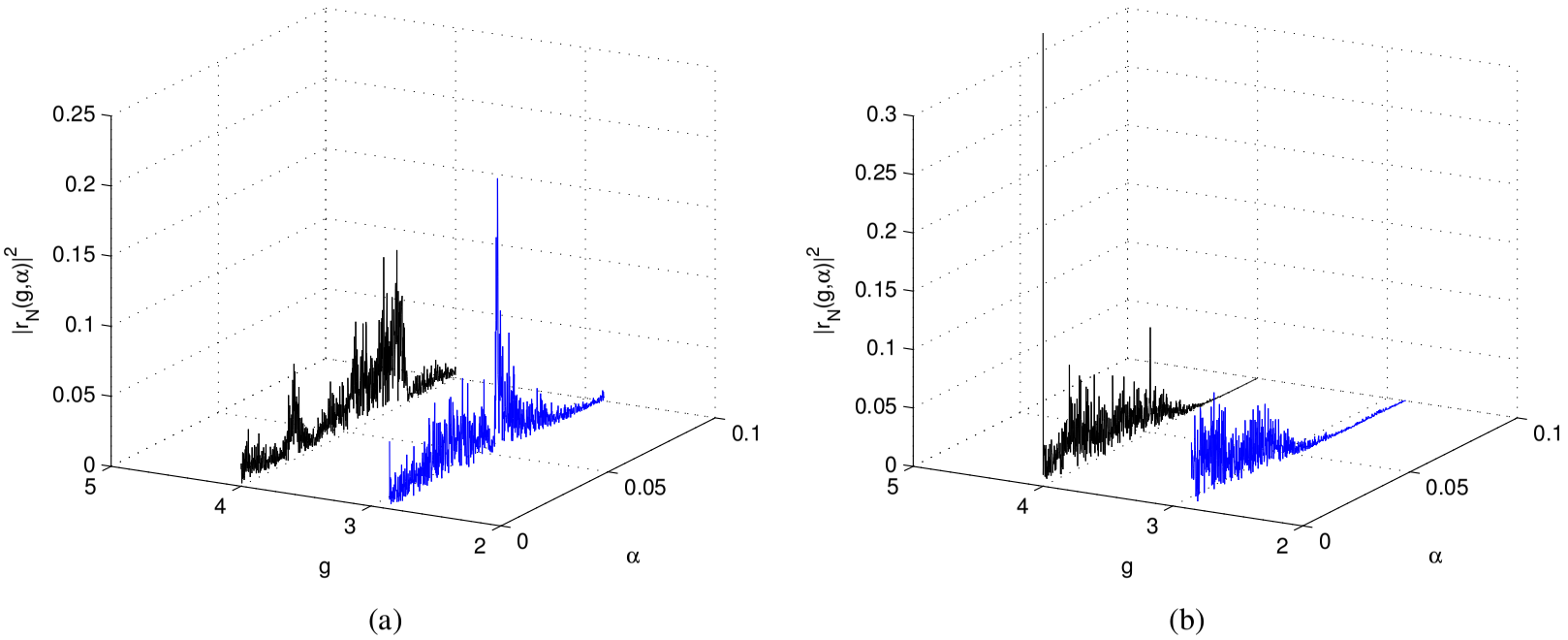

Figure 2: Plots of $|r_N(g_0, \alpha)|^2$ and $|r_N(g_1, \alpha)|^2$ as a function of α for $N = 8192$ at an equivalent sample rate of 20 samples/bit: (a) $|r_N(g_0, \alpha)|^2$ and $r_N|(g_1, \alpha)|^2$ as a function of α when $y(n)$ are samples of PCM/FM; (b) $|r_N(g_0, \alpha)|^2$ and $r_N|(g_1, \alpha)|^2$ as a function of α when $y(n)$ are samples of SOQPSK-TG.

SIMULATION RESULTS

The performance of the algorithm (17) – (19) was simulated using samples of PCM/FM and SOQPSK-TG both at an equivalent sample rate of 20 samples/bit. The maximizations (17) and (18) were carried out using the FFT algorithm to provide a coarse estimate, followed by parabolic interpolation [15] to generate a fine estimate. The interpolated maxima were used for R_0 and R_1. The performance of both the classifier and the bit rate estimator, as a function of signal-to-noise ratio, was simulated.

The first set of plots, given in Figure 3, summarizes the performance of the classifier as a function of signal-to-noise ratio. In the top plot, the $y(n)$ are samples of PCM/FM and is an estimate of the probability of making the correct decision when the true answer is PCM/FM. The bottom plot of Figure 3 is the same except the $y(n)$ are samples of SOQPSK-TG. Thus, the bottom plot is an estimate of the probability of making the correct decision when the true answer is SOQPSK-TG.

The behavior of the classifier when PCM/FM is the true signal is what one might expect. The performance improves as the signal-to-noise ratio increases and as the observation length increases. (The observation length was set to a power of 2 to leverage the computational advantages of the FFT algorithm.) For the simulation parameters used here, the classifier is making essentially error-free decisions when the signal-to-noise ratio is about 15 dB or higher.

The behavior of the classifier when SOQPSK-TG is true signal are somewhat unexpected. At a low signal-to-noise ratio, the classifier makes the correct decision about 50% of the time. In other words, the decision is completely random. As signal-to-noise ratio increases, one expects the situation to improve, but it does not. The probability that the decision is correct *decreases* to near zero before increasing. Close examination of Figure 2 (b) provides possible explanations.

- Because so much of the energy in $|r_N(g_1, \alpha)|^2$ is concentrated at $\alpha = 0$ and because the region immediately around $\alpha = 0$ is omitted from the search, it does not take much noise power to produce a peak in $|r_N(g_0, \alpha)|^2$ that is higher than any peak in $|r_N(g_1, \alpha)|^2$ for $\alpha \neq 0$. This is why the situation improves as signal-to-noise ratio increases above approximately 17 dB.

- The true peak in $|r_N(g_1, \alpha)|^2$ when SOQPSK-TG is true is much narrower than the peak in $|r_N(g_0, \alpha)|^2$ when PCM/FM is true. Consequently, if the coarse search does not have sufficient resolution, the coarse search may entirely miss the true peak. As we implemented it, the resolution of the coarse search increases (improves) as the observation length increases. We believe this is why the performance dramatically improves when the observation length is doubled from 8192 to 16384 samples.

In summary, the classifier (and estimator as described below) requires both sufficiently high signal-to-noise ratio and search resolution to produce useable results.

The second set of plots, shown in Figure 4 summarize the quality of the bit rate estimate used by the classifier. The PCM/FM results are summarized in the top plot of Figure 4. The bit rate estimate error variance decreases as signal-to-noise ratio increases, with a sharp transition in the 12–17 dB range for the simulation parameters used. Above the transition range, the error variance exhibits an error floor. This error variance floor is characteristic of two-step (coarse/fine) estimators based on the DFT [15]. The quality of the bit rate estimate also improves as the length of the observation interval improves: the estimator error variance starts to improve at a lower signal-to-noise ratio and the error variance floor is slightly lower.

The SOQPSK-TG results are summarized in bottom plot of Figure 4. As before, the quality of the estimator improves with with increasing signal-to-noise ratio, and experiences a floor. But here, the influence of coarse search resolution is dramatic. We believe this is due to the ability of the coarse search to correctly identify the true (very narrow) peak in $|r_N(g_1, \alpha)|^2$ when SOQPSK-TG is true. When the true peak can be properly identified, the estimator error variance is very low. This means a very high quality estimate is available.

CONCLUSIONS

PCM/FM and SOQPSK-TG can be reliably distinguished using the methods described in this paper for a sufficiently high signal-to-noise ratio and search resolution. (For the simulation parameters presented here, this signal-to-noise ratio threshold is about 20 dB for an observation length of 16384 samples.) As a byproduct, an estimate of the bit rate is also produced. The quality of this estimate is quite good for sufficiently high signal-to-noise ratio and search resolution. This information (the classifier result and bit rate estimate) can be used to perform pre-flight or pre-launch checks to ensure the telemetry transmitter is properly configured.

ACKNOWLEDGEMENTS

The authors thank Mr. Robert Jefferis, retired from Tybrin Corporation, AFFTC, for providing the motivation for this topic.

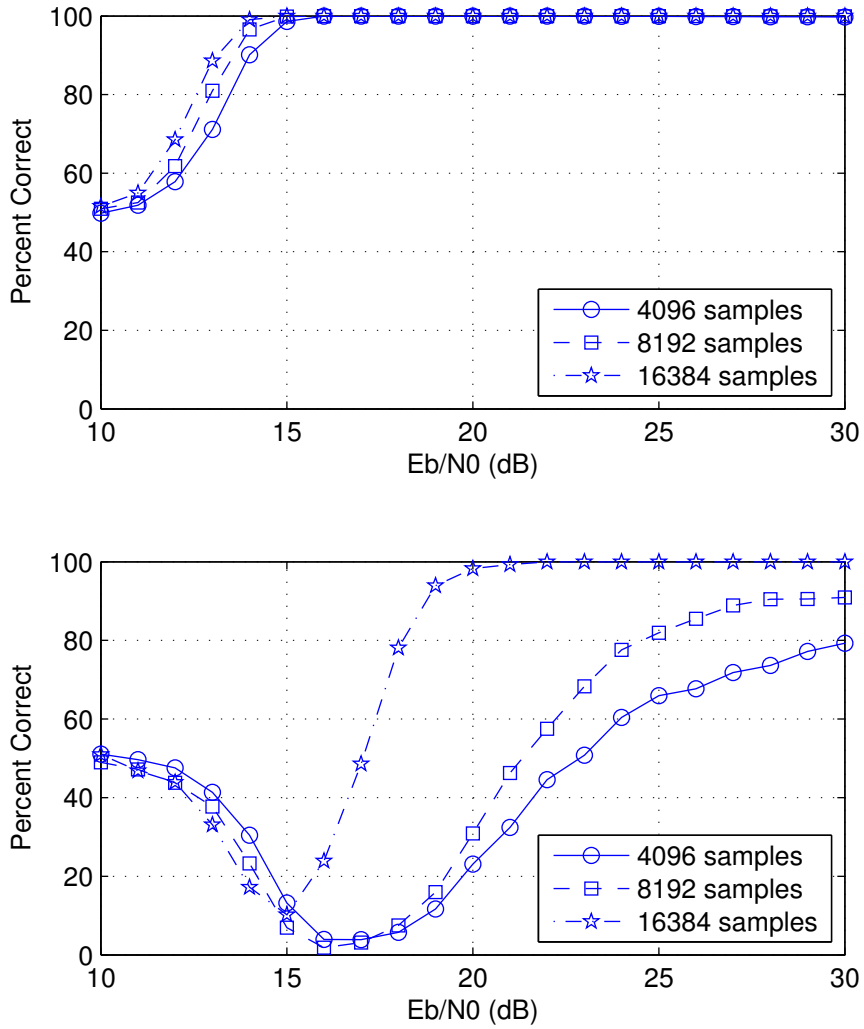

Figure 3: Percent identified correctly when the transmitted signal is PCM/FM (top) and when the transmitted signal is SOQPSK-TG (bottom).

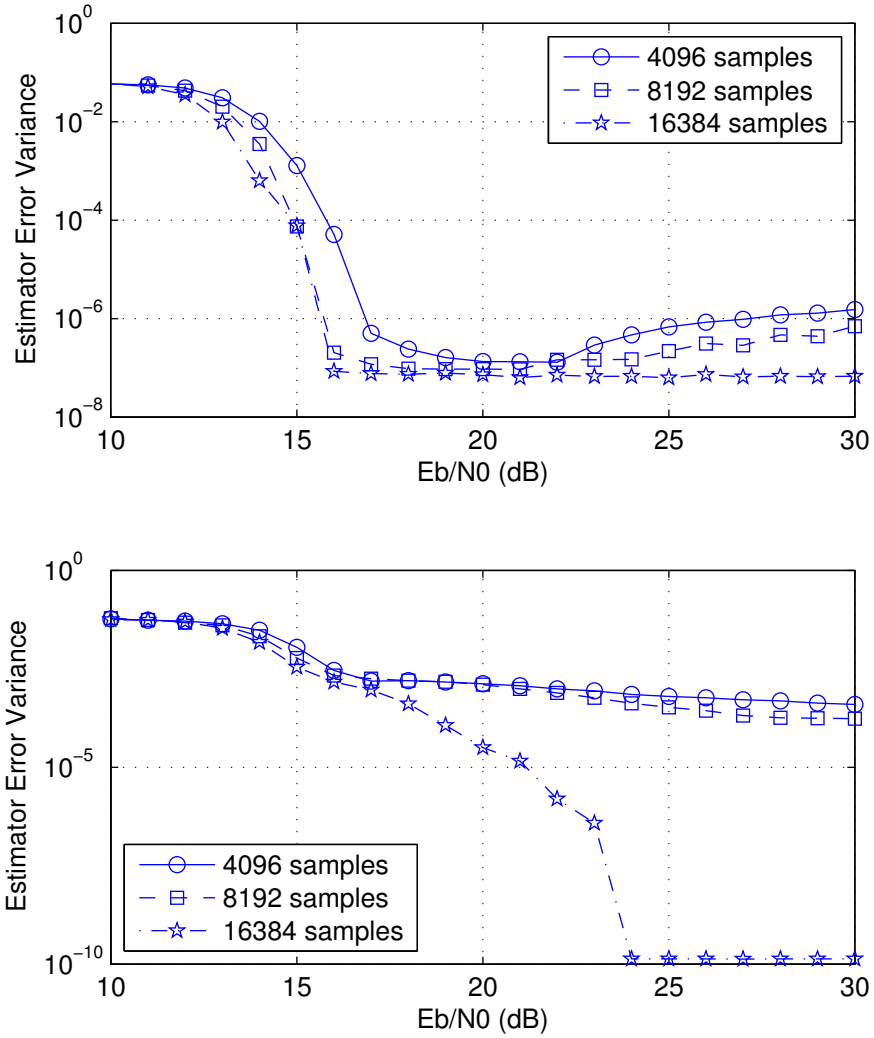

Figure 4: Bit rate estimate variance when the transmitted signal is PCM/FM (top) and when the transmitted signal is SOQPSK-TG (bottom).

REFERENCES

[1] Octavia A. Dobre, Ali Abdi, Yeheskel Bar-Ness, and Wei Su. Blind modulation classification: A concept whose time has come. In *IEEE Sarnoff Symposium on Advances in Wired and Wireless Communication*, pages 223–228, April 2005.

[2] O.A. Dobre, A. Abdi, Y. Bar-Ness, and W. Su. Survey of automatic modulation classification techniques: classical approaches and new trends. *Communications, IET*, 1:137 – 156, 2007.

[3] Tevfik Yucek and Huseyin Arslan. A survey of spectrum sensing algorithms for cognitive radio applications. *IEEE Communications Surveys & Tutorials*, 11:116–130, 2009.

[4] Bassel F. Beidas and Charles L. Weber. Higher-order correlation-based approach to modulation classification of digitally frequency-modulated signals. *IEEE Journal on Selected Areas in Communications*, 13(1):89–101, January 1995.

[5] Bassel F. Beidas and Charles L. Weber. Asynchronous classification of MFSK signals using the higher order correlation domain. *IEEE Transactions on Communications*, 46(4):480–493, April 1998.

[6] S. Kadambe and Q. Jiang. Classification of modulation of signals of interest. In *IEEE Signal Processing Education Workshop*, 2004.

[7] Luca De Vito, Sergio Rapuano, and Maurizio Villanacci. An improved method for the automatic digital modulation classification. In *IEEE International Instrumentation and MeasurementTechnology Conference*, 2008.

[8] Chad M. Spooner. Classification of co-channel communication signals using cyclic cumulants. In *Conference Record of the Twenty-Ninth Asilomar Conference on Signals, Systems and Computers*, 1996.

[9] Chad M. Spooner. On the utility of sixth-order cyclic cumulants for RF signal classification. In *Conference Record of the Thirty-Fifth Asilomar Conference on Signals, Systems and Computers*, volume 1, pages 890–897, 2001.

[10] Christian Dubuc, Daniel Boudreau, Francois Patenaude, and Robert Inkol. An automatic modulation recognition algorithm for spectrum monitoring applications. *IEEE International Conference on Communications*, 1:570–574, 1999.

[11] Antonio Napolitano and Chad M. Spooner. Cyclic spectral analysis of continuous-phase modulated signals. *IEEE Transactions on Signal Processing*, 49(1):30–44, January 2001.

[12] L. Mazet and Ph. Loubaton. Cyclic correlation based symbol rate estimation. In *Conference Record of the Thirty-Third Asilomar Conference on Signals, Systems, and Computers*, volume 2, 1999.

[13] Pascal Bianchi, Phillippe Loubaton, and Francois Sirven. On the blind estimation of the parameters of continuous phase modulated signals. *IEEE Journal on Selected Areas in Communications*, 23(5):944–962, May 2005.

[14] John B. Anderson, Tor Aulin, and Carl-Erik Sundberg. *Digital Phase Modulation*. Plenum Press, 1986.

[15] YV Zakharov, VM Baronkin, and TC Tozer. DFT-based frequency estimators with narrow acquisition range. *IEE Proceedings—Communications*, 148(1):1–7, 2004.